Tail wags the dog is unsupported by biomechanical Modeling of Canidae Tails Use during Terrestrial Motion

Tom Rottier[1,+], Andrew K. Schulz[1,+], Katja Söhnel[2], Kathryn Mccarthy[3], Martin S. Fischer[2], Ardian Jusufi[1,4,5,*]

Locomotion in Bio-robotic and Somatic Systems Group[1]

Max Planck Institute for Intelligent Systems, Stuttgart, Germany

Institut für Zoologie und Evolutionsforschung, Friedrich-Schiller-Universität Jena, Germany[2]

School of Biological Sciences[3]

Georgia Institute of Technology, Atlanta, GA 30332, USA

Swiss Federal Laboratories for Materials Science and Technology[4], Dubendorf Switzerland

Faculty of Science and Engineering[5], Macquarie University, Sydney Australia

December 30, 2022

+ indicates co-first author

Corresponding author:

Ardian Jusufi

Heisenbergstraße 3, Stuttgart, Germany 70569

Keywords:

Mammals, Allometry, Tails

Abstract

Dogs and other members of Canidae utilize their tail for different purposes including agile movement such as running and jumping. One of the unique aspects of the Canidae species is they have a very small size differential as a clade with all of the extant canid species are below 35 kg, except large dog breeds. In this study, we utilize morphological geometries of the animals to test differences in tail use in 24 extant Canidae. We propose evolutionary trade-offs of larger and more massive tails through varying simulations. This work could alleviate unknown biomechanical use of the tails to understand the behavioral biomechanics of lesser-known species in their ability to use their tail for rapid and taxing behaviors including sprinting or climbing. We analyze the phylogenetics between the kinematics of tail use to predicatively hypothesize differences of function for variable center of mass benefits.

Introduction

Canidae is a biomechanically unique clade of species because they are not climbers in their locomotion and are restricted to ground locomotion (Padilla and Hilton, 2015). This is not like all other terrestrial Canivora (except Hyaenidae and the cheetah *Acinonyx jubatus*) (Patel et al., 2016). In addition to greater wrist flexibility, there are significant differences in the tail index, or tail length over body length, with the largest cat tail index of 0.9 in the clouded leopard (Hearn et al., 2013) compared to the cape fox with a tail index of 0.6 (Hunter, 2019). The small tails relative to the body size of Canidae has primary led to the hypothesis that Canidae tails are utilized for agile

ground posture maneuvers such as jumping and turning, much like that of the cheetah (Patel and Braae, 2013; Zhu and Jaroenkunathum, 2022).

Controlling the posture of the body is important in allowing animals to loco mote through complex environments (Biewener et al., 2022; Huang and Ahmed, 2011; Wilshin et al., 2021). For example, in enabling effective acceleration (Hayati et al., 2017; Walter and Carrier, 2009), agile maneuvering and turning (Shield et al., 2021), or attitude control (Fukushima et al., 2021; Jusufi et al., 2010,1; Shield et al., 2021). This is in part due to lizards having long tails with significant inertia such that movements of the tail influence body orientation (Jusufi et al., 2010; Libby et al., 2012). More recently, this effect has also been found in squirrels despite the tail making up a much smaller proportion of total body mass (Fukushima et al., 2021). The tail can have impacts of increasing the moment of inertia in mammals by upwards of 35% (Carrier et al., 2001). Inertia is particularly important in turning as angular momentum can be conserved during mammalian turning (Edwards, 1986). Given the importance that inertia plays in agile locomotion it is valuable to examine the inertial reorientation capabilities of animals with proportionally differing inertia (Walter and Carrier, 2009). It is unknown if larger carnivorans, such as canids, can still use their tails to this effect or whether other appendages, such as head movement, must be used. One such example is in human gymnasts who use the movement of their arms to produce twists (Yeadon, 1993).

Canidae have been shown to exhibit various tail elevations and depressions in different movement paces with many dogs walking with an upright tail whereas galloping with a tail aligned with the spinal column (Kiley-Worthington, 1976). However, these movements are highly complex and require long periods of dedicated practice to be able to perform them, making it an unlikely strategy for other animals. This study sought to design a complex biomechanics model to test the inertial capabilities of canidae tails. The model was compared to that of a previously published study of dogs jumping (Söhnel et al., 2020) and was applied to a greater range of Canidae species to examine inertial differences in tails to discuss potential behavioral implications. The function of the tail as important mean to communicate could be an indirect result, when biomechanics for its use are falsified.

1 Materials & Methods

1.1 Experimental Data of Dog Jumps

The experimental data used for this study were collected from a previous study, Söhnel et al. (2020), where full details of the experimental setup and data collection can be found. Border collies were fitted with a suit containing tracking beads for image analysis and tracking (**Figure 1**A). Border collies performed jumps over a hurdle while kinetics and kinematics were recorded using force plates and a motion capture system (**Figure 1**B). The data were then processed, and the aerial phase separated out before joint kinematics were calculated (**Figure 1**C-D).

To deal with missing marker data, cubic smoothing splines were fitted to the data with any missing values removed. The splines were then evaluated over the original time to give a data set with no missing data. The amount of smoothing was determined through trial and error until a good fit to the data was found through visual inspection. For some markers there were gaps at the beginning and end of the trial, however, they will not affect this analysis as only the middle portion of the trial, during the aerial phase, was used for further analysis.

Take-off was determined as follows. First, the variability in the force signal was determined by calculating the average standard deviation in force across all force plates that were unloaded during the trial. Then the total vertical force acting on the dog was calculated by summing the vertical

force across all force plates. Take-off was finally taken to be the first moment that the summed vertical force exceeded zero minus twice the calculated variability (as applied forces are negative). The experimental setup meant that a hurdle was resting on one of the force plates, the data from this force plate was thus subtracted from the total vertical force. The same approach was used to determine touchdown, and thus extract the aerial phase.

1.2 Kinematics of Dog Flight Experiments

The dog was represented by 17 segments comprising the head, neck, upper torso, lower torso, upper limb, lower limb and paw for each limb, and tail corresponding to the tracker beads from the study (**Figure 1**A). Local coordinate systems were then defined for each segment as follows: the longitudinal (z) axis was the vector joining the proximal and distal joint centers, the vertical (y) axis was the cross product of the z axis and a vector joining and medial to lateral marker, the mediolateral (x) axis was then the cross product of the y and z axes.

As no first-hand information was available, the inertial parameters of the segments (mass, moment of inertia, center of mass location) were taken from a variety of sources. Relative values were taken from Amit et al. (2009) (Amit et al., 2009), who determined these for three breeds of dogs of differing sizes, using MRI. However, their data combined the upper and lower torso inertia and did not include the tail. Those segments were therefore modelled as solid cylinders, the lengths of these segments were taken from the data, but the radii were estimated at 20 cm, 20 cm, and 2 cm for the upper and lower torso and tail, respectively. The masses of the torso segments were determined from CT scans performed on a dog of the same breed and for the tail the relative value was taken from Jones et al. (2018) (Jones et al., 2018). Using the parameters in this model we viewed the entire dog and the tail scale kinematics during the jump (**Figure 1**C-D). Utilizing this we viewed the tail as a body and viewed the rotation in the three axes of the center of mass including about the z (roll), about the y (yaw), and about the x (pitch) (**Figure 1**E-F).

1.3 Scaling of Canidae Tail Movement

To compare jumping ability among Canidae, we will report the relationship between tail length, body length, and body mass for $n = 24$ extant members of the Canidae family as well as a power law best fit that describes the trend (**Figure 3**A). Due to data deficiencies we had to exclude certain $n = 10$ extant members of the Canidae family including many of the smaller species due to data large gaps of data including *Nyctereutes procyonoides viverrinus* or the Japanese Raccoon Dog, the full list of species studied can be found on the cladogram in **Figure 4**B and **Table S1**. As part of the scaling of these species we include analysis of the tail index. The tail index can be described by the following Equation:

$$TI = \frac{L_{tail}}{L_{body}} \tag{1}$$

where L_{tail} is the length of the dog tail L_{body} is the body length of the body, given in meters. Body length was normalized to be from the nose of the head to the end of the torso. Therefore, the effective total length of the species could be described as the sum of these two lengths.

1.4 Phylogenetics Comparison of Species

We hypothesize that the trend is due to phylogenetic dependence between the nine species studied. To determine the extent that our trends are influenced by phylogenetic closeness, we performed a Phylogenetic Independence Contrasts (PIC) analysis, a statistical method controlling for the

effects of phylogeny (Felsenstein, 1985). Our analysis of canids included body mass versus tail length, body length, and tail index is indicated in **Table S1**. We began by generating a consensus phylogeny using pruned subsets from VertLife including all 24 species(**Figure 3**B) (Upham et al., 2019). Using the *pic* function and the package *ape* in R studio. We performed PIC analysis for four different scaling factors including tail length versus body mass, body length versus body mass, angle magnitude versus body mass, and tail index versus body mass.

2 Mathematical Modeling

The modelling approach here was similar to Yeadon et al., (1990) in their study on aerial motions in humans (Yeadon, 1990). The model matched the one used with the experimental data and therefore also had 17 segments comprising the head, neck, upper torso, lower torso, upper, lower, and paw for each of the four limbs, and tail. Each upper limb joint center was displaced from the corresponding joint on the back by a constant amount that was determined from taking the mean vector between the two joint centers expressed in the upper limbs local coordinate system, which remained roughly constant throughout the jump. Separate values were used for the fore and hind limbs. The inertial parameters of each segment were the same as those used with the experimental data.

Each segment had three degrees of freedom (DoF) which were the three Euler angles (pitch-yaw-roll rotation sequence) parameterizing the rotation of a reference frame fixed in the parent segment to one fixed in the segment. The upper torso segment defined the overall orientation of the model, with its DoF specifying the rotation of its frame from the fixed, laboratory frame. Parent frames started from the upper torso segment and proceeded out from proximal to distal segments. The model was kinematically driven in that the orientation angles for each segment were specified as functions of time. This reduced the model to just three DoF which were the three angles specifying the overall orientation of the model. The functions specifying the rest of the segment's orientation were quintic splines fitted to the experimental data, as these also gave the first and second derivatives, with respect to time, of the angles by differentiating the coefficients.

2.1 Simulations

The model was given initial conditions determined from the data which were the angles and angular velocity of the upper torso at the start of the aerial phase. The kinematic and dynamic equations of motion were then integrated forward in time for the duration of the aerial phase determined from the trial (0.293 s) to produce time-histories for the three upper torso orientation angles.

Given the uncertainty in the model parameters, ensemble simulations were performed whereby multiple simulations were performed each with the parameters varied slightly. For each ensemble simulation, 1000 individual simulations were performed each with the model's parameters randomly drawn from a uniform distribution from $\pm$ 20% of the original value. The mean and 5-95% quartiles for the simulations were then calculated.

An optimization was also performed on the parameters to minimize the mean squared (MSE) difference between the experimental data and the simulation.To do so, an evolutionary algorithm was used to vary the parameters to minimize a cost function comprising the sum of the mean squared error in the time histories for each of the orientation angles. Bounds were set to $\pm$ 10% of the original values. The optimization was then repeated with the bounds increased to 20% to see what effect a larger change in parameters would have on the outcome.

The ability to control the movement of each segment now meant we could explore the effects of different movements on the orientation of the model. Two alternative movement schemes were used:

one where the segments were fixed at their orientation at take-off, and one where the orientation angles were linearly interpolated between the angles at take-off and touchdown (taken from the experimental data). Simulations were then re-run with everything the same except for the altered segment orientations. Simulations were performed using both schemes for: all segments, only the lower torso, the tail, the combined fore and hind limbs, and all joints except the lower torso.

All simulations were performed in the Julia (Bezanson et al., 2017) using the SciML ecosystem (Rackauckas and Nie, 2017).

Modeling of Canidae Tree

Utilizing the scaling measurements from the previous section, we developed a scaling factor for each of the species using the ratio between the masses. Assuming isometric scaling across the limbs allows us to approximate the limb length for the model constraints with the limb lengths scaling by $m^{1/3}$ (Campione and Evans, 2012) and limb moments of inertia by $m^{5/3}$ as given by current mammalian literature (Kilbourne and Hoffman, 2013). The tail scale factor determined is $S_1 = \frac{L}{L_0}$ with the tail mass scaling as s_1^3 and moment of inertia as s_1^5. To determine the scale factor for the rest of the body we utilize the Equation:

$$s_2 = \frac{M - m_{T_o}(\frac{L}{L_0})^3}{\sum_i m_{i_0}} \tag{2}$$

with the lengths scaling as $s_2^{1/3}$ and the moment of inertia as $s_2^{5/3}$. As this allows the overall body mass to remain the same with a differently proportioned tail.

We input the mass of the species with the given average body length, L_{body}, tail length L_{tail}, and body mass m along with the assumptions of isometric scaling to calculate impulse control. For each of the species, we viewed the maximum absolute difference in the three axes of rotation with the rotation about the x-axis as roll, rotation about the y-axis yaw, and rotation about the z-axis as pitch (**Figure 1**E) for each of the canidae species (**Figure 4**A).

To normalize the variance in the pitch, yaw, and roll we utilized the maximum absolute difference in radians, MAD which is calculated as the difference from the original simulation:

$$\Delta\theta_{yaw} = |\theta_{yaw,simmax} - \theta_{yaw,simmin}| \tag{3}$$

$$\Delta\theta_{pitch} = |\theta_{pitch,simmax} - \theta_{pitch,simmin}| \tag{4}$$

$$\Delta\theta_{roll} = |\theta_{roll,simmax} - \theta_{roll,simmin}| \tag{5}$$

where all values are in radians. Utilizing each of these maximum differences, we take the magnitude of the vector for each given by the angle magnitude, $\|\theta\|$, calculated as

$$\|\theta\| = \sqrt{(\Delta\theta_{yaw})^2 + (\Delta\theta_{pitch})^2 + (\Delta\theta_{roll})^2}. \tag{6}$$

The angle magnitude, θ is given in units of radians.

3 Results

Model Case Study of *Canis lupus familiaris*

Using joint angle time histories from the experimental data of Söhnel et al. (2020) allows us to evaluate the model by comparing the simulation outputs to the data in **Figure 1**F, with the shaded regions showing the 5th-95th percentile for the ensemble simulations and the solid line showing the mean. The average RMSE for the three orientation angles was 0.0673 rad (4 degrees). The optimization with bounds at 10% only decreased the RMSE slightly by 0.1 degrees and the optimization with bounds at 20% decreased the RMSE by 0.8 degrees. The majority of parameters changed in the same direction (increased or decreased) between the two optimization. All optimization converged within 300 generations.

When specifying the time histories for specific joints, or subsets of joints, the largest effect on the orientation angles came from controlling the joint between the upper and lower torso. This resulted in a difference in pitch, yaw, and roll angles of 0.685 rad (39.2 degrees), 0.136 rad (7.78 degrees), and 0.259 rad (14.7 degrees), respectively, at the end of the simulation between the original and with the lower body fixed. Similar but slightly smaller differences were observed when the joint angles were linearly interpolated (**Figure S4A**). When controlling the fore and hind limbs or tail, there was no observable difference in orientation angles (**Figure S4B**), in fact when controlling all joints except the torso joint there was only a small difference in the joint angles (**Figure S4C**).

Scaling of Tail Biomechanical Impact across Canidae

We collected n = 35 species of Canidae morphometrics measurements including tail length(Berta, 1982; Burnie, 2005; Dietz, 1984; Geptner et al., 1988; Hoffman, 2014), body length(Bekoff, 1977; de Waal, 2017; Hoffman, 2014; Hunter, 2019; Viranta et al., 2017), and body mass(Padilla and Hilton, 2015). These studies are a range of measurements including field measurements of exotic canids as well as veterinary measurements of more well known and domesticated species.

We begin with the hypothesis that the tail length of Canidae are isometric: their proportions do not change with body size.

Limb length has long been described to scale at slopes of 0.33 and for Canidae we see that the tail length scales:

$$L_{tail} = 0.24m^{0.14} \tag{7}$$

With the exponent being less than 0.18 we see commonality compared to that of other terrestrial species. **Figure 3** shows the relationship between body mass and tail length for the Canidae species. Furthermore, we find that the tail index given by Equation (1) has negative allometry given by the Equation:

$$TI = 0.66m^{-0.23} \tag{8}$$

indicating a negative logarithmic degradation for increased masses (**Figure 3**B). The tail index is normalized by body length over tail length. Each of these allometries is governed by scaling to 1/3 and therefore the ratio of the length of tail and body length should be isometric. There was not enough morphological data on several species and therefore for the angular models we only viewed 24 canidae species. Utilizing these length scale relationships when we view the simulations of the yaw, pitch, and roll of the species we see a large variance in each of the species with the magnitudes of the angles (**Figure 4**A). We capture the maximum absolute difference of each of the three axes of rotations pitch, yaw, and roll utilizing Equation (3-5) respectively we separate these into the species of studied Canidae with their maximum absolute difference in **Figure 4**B-C. Taking the magnitude of these species differentiation we can detect which canids have the largest deformation

from our model by viewing the magnitude change caused by the tail using Equation (6) we find that the angle magnitude scales negatively in respect to tail index with the Equation:

$$\theta = 0.16(TI)^{-1.28} \tag{9}$$

and with respect to body mass:

$$\theta = 0.20m^{0.505}. \tag{10}$$

The trend of Equation (9) is displayed in **Figure 5**A, and the trend of Equation (10) is displayed in **Figure 5**B. In these Equations θ is given in radians and we see larger canids have larger angle magnitudes however in reference to the tail index this is decreasing at a nearly linear rate. With respect to phylogenetic dependence of these relationships, we utilize phylogenetic independence correlation (PIC) as described in methods to detect if any of these scaling relationships are due to evolutionary similarity. We found that the tail length PIC and body mass PIC are not related, and thus phylogenetic dependence of our sample was significant (p=0.005; **Figure S1A**). We proceed to find the phylogenetic dependence with respect to body length is significant (p=0.003; **Figure S1B**).

We repeat the above method for the power law trend found between maximum absolute difference and body mass using the same consensus phylogeny of $n = 24$ species. We found that tail index PIC and body mass PIC are not related, and thus phylogenetic dependence of our sample was not significant (p=0.46; **Figure S2**). Finally, we analyze the PIC of the maximum absolute difference versus body mass and find that they are not related, and thus the phylogenetic dependence of our sample was significant ($p=2.37\cdot10^{-7}$).

Genus Differentiation

The Canidae species has large genera groups including *Canis, Lycalopex, and Vulpes*. Each of these was examined in their differentiation and of magnitude values of *Vulpes*, $\theta = 0.39 \pm 0.19$ radians, *Lycalopex*, $\theta = 0.40 \pm 0.09$ radians, and *Canis*, $\theta = 0.88 \pm 0.2$ radians. In doing a two tailed t-test with variance of means we find statistical significance $p = 0.0012$ between *Canis* and *Lycalopex* and $p = 0.0014$ between *Canis*s and *Vulpes* in respect to the angle magnitude (**Figure 5**C).

Discussion

Scaling of Canid Tails

We see very surprising results of the tail scaling of the canids as compared to other terrestrial taxa as they are nearly equal to that of many other mammals Weisbecker et al. (2020). The scaling of climbing mammals (scansorial and arboreal mammals) scales at much higher rates as larger mammals including big cats and monkeys utilize their tails for substrate attachment for assistance in climbing (Organ et al., 2011).

The small amount of tail biomechanical impact on the center of mass could indicate that the tail use is even less present in terrestrial locomotion than in other terrestrial species. The mass scaling indicates that the wolf (*Canis lupus*), the largest of the canids studied at 35-80kg, has only a 10 cm longer tail than the Velox fox (*Vulpes velox*), which weighs just 2.1 kg. It should also be mentioned that the fox has nearly three to four times the body length of the Velox fox. Tail use in the dogs could have evolved to be more specialized in specific species. Across Canids it appears the inertial impacts that tail movement has on complex maneuvers such as jumping, have little to no effect.

Tail Behavioral and Biomechanical Implications

In many mammalian species, tails are critical for their biomechanics, but the results of this model display that tails contribute little to the biomechanics of canids. Tail movement is critical in agile movements of the cheetahs during rapid movements, such as hunting where their high inertia tail allows rapid turning of nearly $190\frac{^\circ}{s}$ during prey chases (Hudson, 2011; Wilson et al., 2013). However the fastest of the studied canids is the wolf, which reaches speeds of 13 m/s whereas a cheetah is nearly three times that speed. Cheetahs have been compared to similar the sized greyhound which only reaches a top speed of 17 m/s(Hudson et al., 2012). Felidae and other tailed animals are also different in distributing more of their body mass to the hind limbs allowing more generation of tail inertia(Wilson et al., 2013). The precision of the model in reference to the movement of the dog displays, that the tail of the dog has minimal impact on the center of mass movement during the jump which indicates in fact that Canidae tails are not primarily used for biomechanics.

Dogs seem to utilize their tails for different behavioral communication(Hecht and Horowitz, 2015), and canids have been shown to respond more positively to tail wagging as a social cue for *friendliness*(Reimchen and Leaver, 2008). Another explanation could be the use in pest control with tails acting to ward off flies or other animals (Matherne et al., 2018). Tails can operate in a behavioral sense as well in marking behavior like in the African Wild Dog(Parker, 2010).

There are many online platforms that indicate that dogs utilize their tails for complex maneuvers such as turning and jumping, but given the incredibly low angular movement, the tail is imposing on the center of mass in a range of canid species we believe at this point, that the dog tail is primarily adapted for communication with the length growing at an incredibly small rate of nearly $m^0.14$. Pretending that further study of smaller dog tail morphologies will confirm our findings, it is possible this scaling could be nearly isometric We also see that for larger body lengths the tail decreases in size giving a smaller tail index. It has been hypothesized that faster canids utilize longer tails for counterbalances, but we see contrasting evidence in this scaling as well as based on the angle magnitude model.

Model Limitations

There are limitations in the data access of the canid species. Many of the smaller Canidae species have only been documented through hand drawn images and there is almost no morphological data present at all for some of the rare and endangered species. Further study is needed on the Canidae biomechanics as well as there is no biomechanics literature present on the Canidae movement outside of varying species of domesticated dogs.

The modeling portion of this paper utilizes a complex biomechanical model of the dog and analyze how different movements of the joints affected the outcome. Initially the model could be evaluated against the experimentally collected data on the dogs when the same joint movements were input. The close match of the model to the data in **Figure 1**F, $RMSE < 4^\circ$, indicates it represented the dog quite well. Any discrepancy between the model and the data can either be due to the model itself being wrong, the parameters, or the inputs (the joint angle time histories). It is most likely the error comes from the parameters as they had to be estimated; the mode, while still making assumptions about rigidity and segment definitions, is likely complex enough, and the inputs will contain only small amounts of error. Relative values had to be taken for most segments as data for the breed of dog used is not available, geometric modelling was also used for some segments where relative values could not be found. Overall, given the good match between simulation and data these limitations do not likely affect the conclusions.

Conclusion

The Canidae have different types of movement patterns, however all of these patterns are on the ground. Dogs have been described as utilizing their tails for agile moments such as jumping or running. We tested this hypothesis using a 17 degree of freedom model implemented on 25 different Canidae species. We find that larger Canidae have larger tails however the tail index ratio decreases for larger species, such as wolves. The utilizing of the tail during jumping mechanisms achieves very low amounts of center of mass movement across all species with the largest being under a single degree. We believe that this implies that dogs utilize their tails for other means, such as communication and pest control, but not for agility in maneuvers.

Acknowledgements

We wish to thank the entire Fischer group for sharing their data and methodologies with our team. We thank Amir Patel for his insights into our mechanical model and his assistance in interpreting results.

Competing Interests

The authors declare no conflicts of interest in any of this manuscript.

Funding Statement

This project was supported by a Max Planck and Cyber Valley grant to A.J. (grant Nr. CyVy-RF-2019-08). K.S. and M.S.F. were supported by Gesellschaft zur Förderung kynologischer Forschung e.V.

Data Access Statement

We have included files for the modeling experiment as well as all of the scaling data which is included in the supplementary information including lengths as well as where the scaling data was pulled from.

Ethics Statement

All data was accessed from a previously published article that collected all items with ethical clearance. Information on the ethical information is provided in the Söhnel et al. text(Söhnel et al., 2020).

References

Amit, T., Gomberg, B., Milgram, J., and Shahar, R. (2009). Segmental inertial properties in dogs determined by magnetic resonance imaging. *The Veterinary Journal*, 182(1):94–99.

Bekoff, M. (1977). Canis latrans. *Mammalian Species*, (79):1–9.

Berta, A. (1982). Cerdocyon thous. *Mammalian Species*, (186):1–4.

Bezanson, J., Edelman, A., Karpinski, S., and Shah, V. B. (2017). Julia: A fresh approach to numerical computing. *SIAM review*, 59(1):65–98.

Biewener, A. A., Bomphrey, R. J., Daley, M. A., and Ijspeert, A. J. (2022). Stability and manoeuvrability in animal movement: lessons from biology, modelling and robotics. *Proceedings of the Royal Society B: Biological Sciences*, 289(1967):20212492. Publisher: Royal Society.

Burnie, D. (2005). *Animal: The Definitive Visual Guide to the World's Wildlife*. DK, Washington, D.C. : New York, 1st edition edition.

Campione, N. E. and Evans, D. C. (2012). A universal scaling relationship between body mass and proximal limb bone dimensions in quadrupedal terrestrial tetrapods. *BMC Biology*, 10(1):60.

Carrier, D. R., Walter, R. M., and Lee, D. V. (2001). Influence of rotational inertia on turning performance of theropod dinosaurs: clues from humans with increased rotational inertia. *Journal of Experimental Biology*, 204(22):3917–3926.

de Waal, H. (2017). Demography and morphometry of blackbacked jackals Canis mesomelas in South Africa and Namibia. *ALPRU-Occasional Paper*.

Dietz, J. M. (1984). Ecology and social organization of the maned wolf (Chrysocyon brachyurus). Accepted: 2008-07-22T20:42:32Z.

Edwards, M. H. (1986). Zero angular momentum turns. *American Journal of Physics*, 54(9):846–847. Publisher: American Association of Physics Teachers.

Felsenstein, J. (1985). Phylogenies and the Comparative Method. *The American Naturalist*, 125(1):1–15.

Fukushima, T., Siddall, R., Schwab, F., Toussaint, S. L. D., Byrnes, G., Nyakatura, J. A., and Jusufi, A. (2021). Inertial Tail Effects during Righting of Squirrels in Unexpected Falls: From Behavior to Robotics. *Integrative and Comparative Biology*, 61(2):589–602.

Geptner, V. G. V. G., Nasimovich, A. A., Bannikov, A. G., and Hoffmann, R. S. (1988). *Mammals of the Soviet Union*. Washington, D.C. : Smithsonian Institution Libraries and National Science Foundation.

Hayati, H., Eager, D., Jusufi, A., and Brown, T. (2017). A Study of Rapid Tetrapod Running and Turning Dynamics Utilizing Inertial Measurement Units in Greyhound Sprinting. American Society of Mechanical Engineers Digital Collection.

Hearn, A. J., Ross, J., Pamin, D., Bernard, H., Hunter, L., and Macdonald, D. W. (2013). Insights into the Spatial and Temporal Ecology of the Sunda Clouded Leopard Neofelis Diardi. page 6.

Hecht, J. and Horowitz, A. (2015). Introduction to dog behavior. page 26.

Hoffman, M. (2014). IUCN Red List of Threatened Species: Canis adustus. *IUCN Red List of Threatened Species*.

Huang, H. J. and Ahmed, A. A. (2011). Tradeoff between stability and maneuverability during whole-body movements. *PloS One*, 6(7):e21815.

Hudson, P. E. (2011). *The structural and functional specialisation of locomotion in the cheetah (Acinonyx Jubatus)*. Ph.D., Royal Veterinary College (University of London). Accepted: 2011.

Hudson, P. E., Corr, S. A., and Wilson, A. M. (2012). High speed galloping in the cheetah (Acinonyx jubatus) and the racing greyhound (Canis familiaris): spatio-temporal and kinetic characteristics. *Journal of Experimental Biology*, 215(14):2425–2434.

Hunter, L. (2019). *Carnivores of the World: Second Edition*. Princeton University Press. Google-Books-ID: ydOOtgEACAAJ.

Jones, O. Y., Raschke, S. U., and Riches, P. E. (2018). Inertial properties of the German Shepherd Dog. *PLOS ONE*, 13(10):e0206037. Publisher: Public Library of Science.

Jusufi, A., Kawano, D. T., Libby, T., and Full, R. J. (2010). Righting and turning in mid-air using appendage inertia: reptile tails, analytical models and bio-inspired robots. *Bioinspiration &amp$\mathsemicolon$ Biomimetics*, 5(4):045001. Publisher: IOP Publishing.

Jusufi, A., Zeng, Y., Full, R. J., and Dudley, R. (2011). Aerial Righting Reflexes in Flightless Animals. *Integrative and Comparative Biology*, 51(6):937–943.

Kilbourne, B. M. and Hoffman, L. C. (2013). Scale Effects between Body Size and Limb Design in Quadrupedal Mammals. *PLoS ONE*, 8(11):e78392.

Kiley-Worthington, M. (1976). The Tail Movements of Ungulates, Canids and Felids with Particular Reference to Their Causation and Function as Displays. *Behaviour*, 56(1/2):69–115. Publisher: Brill.

Libby, T., Moore, T., Chang-Siu, E., Li, D., Cohen, D., Jusufi, A., and Full, R. (2012). Tail-assisted pitch control in lizards, robots and dinosaurs. *Nature*, 481:181–4.

Matherne, M. E., Cockerill, K., Zhou, Y., Bellamkonda, M., and Hu, D. L. (2018). Mammals repel mosquitoes with their tails. *Journal of Experimental Biology*, 221(20):jeb178905.

Organ, J. M., Muchlinski, M. N., and Deane, A. S. (2011). Mechanoreceptivity of Prehensile Tail Skin Varies Between Ateline and Cebine Primates. *The Anatomical Record*, 294(12):2064–2072.

Padilla, L. R. and Hilton, C. D. (2015). Canidae. *Fowler's Zoo and Wild Animal Medicine, Volume 8*, pages 457–467.

Parker, M. N. (2010). *Territoriality and scent marking behavior of African wild dogs in northern Botswana*. Ph.D., University of Montana, United States – Montana. ISBN: 9781124068350 Publication Title: ProQuest Dissertations and Theses.

Patel, A., Boje, E., Fisher, C., Louis, L., and Lane, E. (2016). Quasi-steady state aerodynamics of the cheetah tail. *Biology Open*, 5(8):1072–1076.

Patel, A. and Braae, M. (2013). Rapid turning at high-speed: Inspirations from the cheetah's tail. In *2013 IEEE/RSJ International Conference on Intelligent Robots and Systems*, pages 5506–5511. ISSN: 2153-0866.

Rackauckas, C. and Nie, Q. (2017). Differentialequations.jl–a performant and feature-rich ecosystem for solving differential equations in julia. *Journal of Open Research Software*, 5(1):15.

Reimchen and Leaver (2008). Behavioural responses of Canis familiaris to different tail lengths of a remotely-controlled life-size dog replica. *Behaviour*, 145(3):377–390.

Shield, S., Jericevich, R., Patel, A., and Jusufi, A. (2021). Tails, Flails, and Sails: How Appendages Improve Terrestrial Maneuverability by Improving Stability. *Integrative and Comparative Biology*, 61(2):506–520.

Söhnel, K., Rode, C., de Lussanet, M. H. E., Wagner, H., Fischer, M. S., and Andrada, E. (2020). Limb dynamics in agility jumps of beginner and advanced dogs. *The Journal of Experimental Biology*, 223(Pt 7):jeb202119.

Upham, N. S., Esselstyn, J. A., and Jetz, W. (2019). Inferring the mammal tree: Species-level sets of phylogenies for questions in ecology, evolution, and conservation. *PLOS Biology*, 17(12):e3000494.

Viranta, S., Atickem, A., Werdelin, L., and Stenseth, N. C. (2017). Rediscovering a forgotten canid species. *BMC Zoology*, 2(1):6.

Walter, R. M. and Carrier, D. R. (2009). Rapid acceleration in dogs: ground forces and body posture dynamics. *Journal of Experimental Biology*, 212(12):1930–1939.

Weisbecker, V., Speck, C., and Baker, A. M. (2020). A tail of evolution: evaluating body length, weight and locomotion as potential drivers of tail length scaling in Australian marsupial mammals. *Zoological Journal of the Linnean Society*, 188(1):242–254.

Wilshin, S., Reeve, M. A., and Spence, A. J. (2021). Dog galloping on rough terrain exhibits similar limb co-ordination patterns and gait variability to that on flat terrain. *Bioinspiration & Biomimetics*, 16(1):015001.

Wilson, A. M., Lowe, J. C., Roskilly, K., Hudson, P. E., Golabek, K. A., and McNutt, J. W. (2013). Locomotion dynamics of hunting in wild cheetahs. *Nature*, 498(7453):185–189. Number: 7453 Publisher: Nature Publishing Group.

Yeadon, M. (1993). The biomechanics of twisting somersaults Part III: Aerial twist. *Journal of Sports Sciences*, 11(3):209–218.

Yeadon, M. R. (1990). The simulation of aerial movement—II. A mathematical inertia model of the human body. *Journal of Biomechanics*, 23(1):67–74.

Zhu, J. and Jaroenkunathum, C. (2022). Enabling Robots to Jump like Dogs.

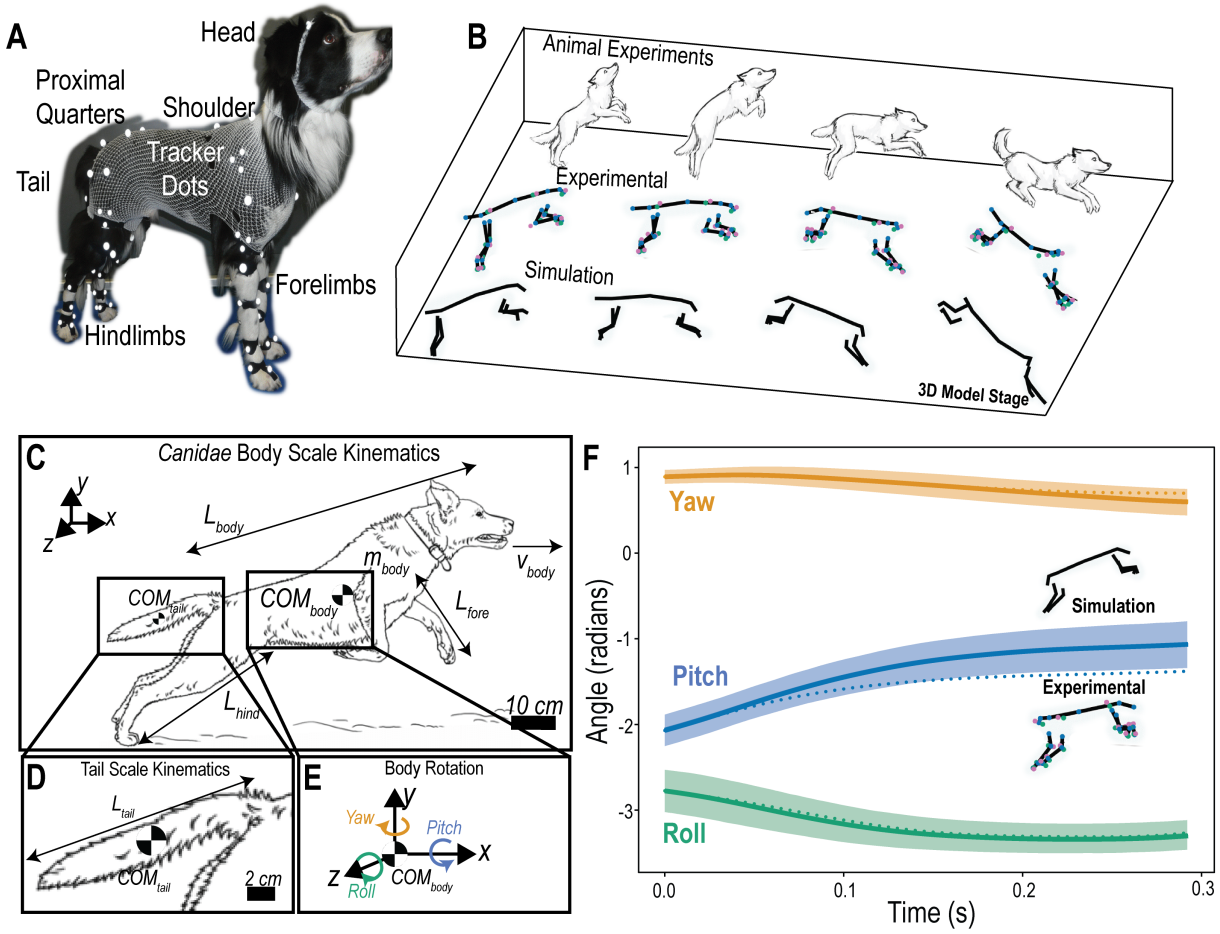

Figure 1: A) Experimental set up for data collection. B) Sequences of reconstructed movements from Animal Experiment, experimental joint tracking, and simulation. C) Body Scale Kinematics Measurements. D) Tail Scale Kinematics Measurements. E) Body Rotation Axis indicating Yaw in the positive y axis, roll in the positive x axis, and pitch in the positive z axis. F) Comparison of orientation angles between experimental data (dotted) and simulated (solid). Shaded region is the 5-95% quartiles for the ensemble simulation. Illustrations from Adobe stock open source drawings.

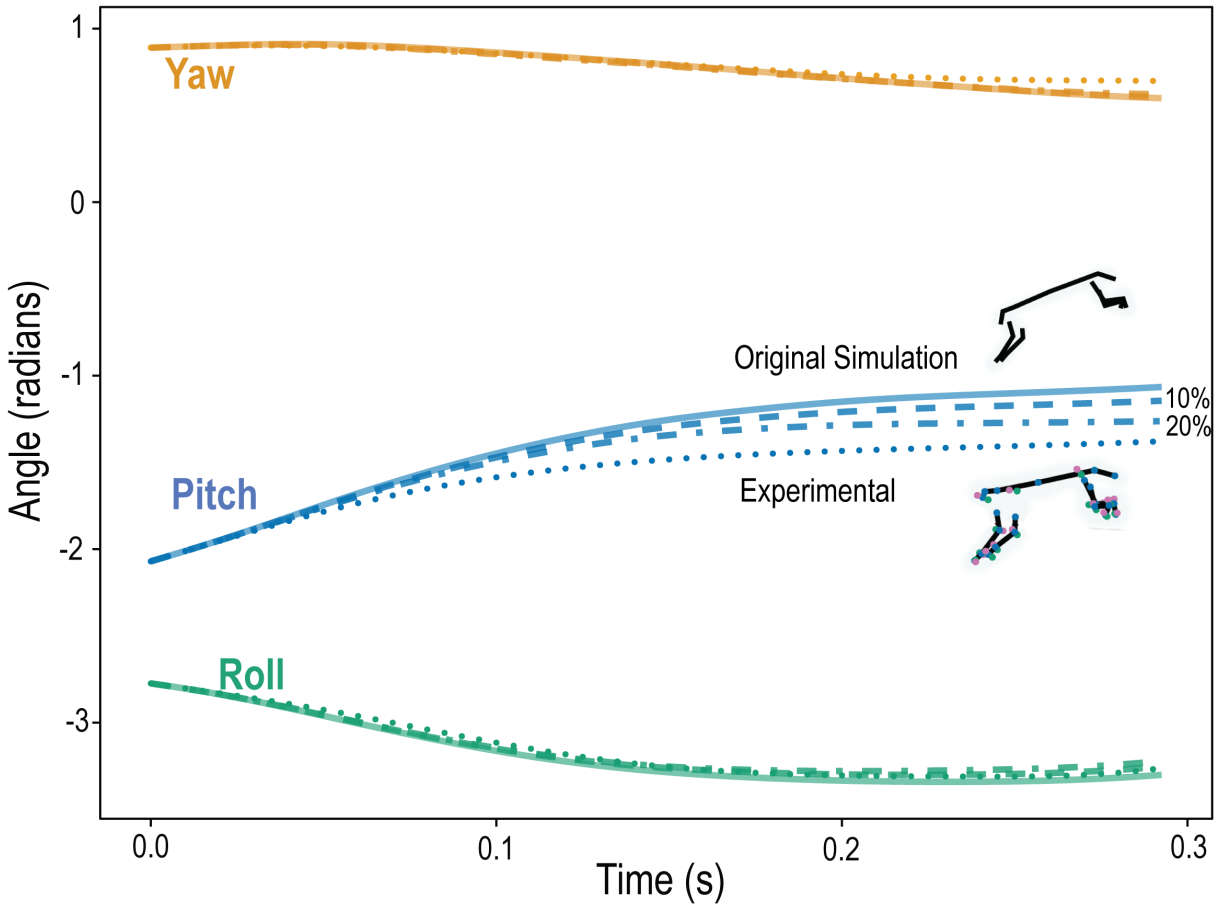

Figure 2: A) Orientation angles for the original simulation (solid line), optimized with 10% bounds (dashed line), optimized for 20% bounds (dashed-dot line), and experimental data (dotted line)

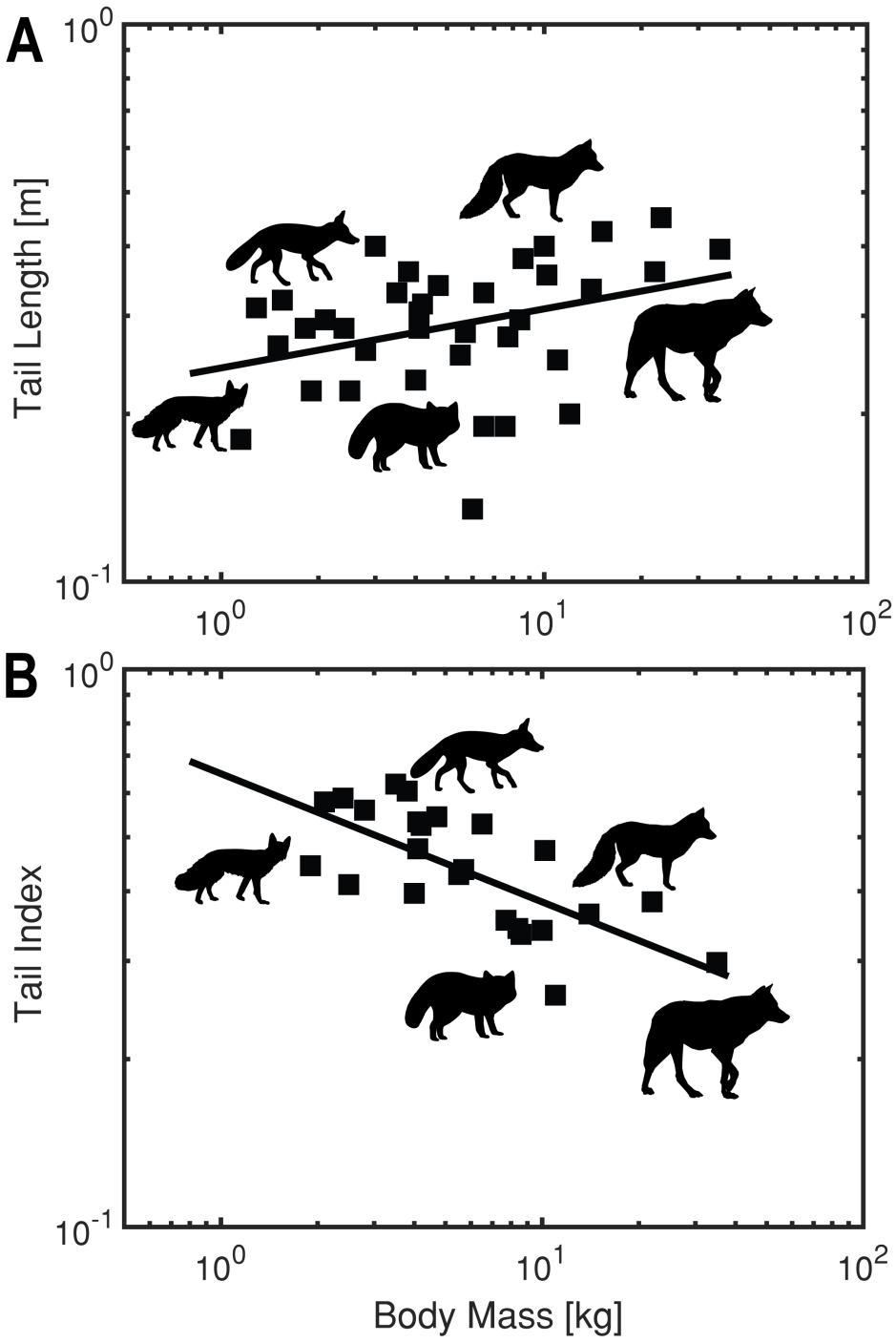

Figure 3: Scaling of Tail Length in m of $n = 35$ different *canidae* species versus body mass in kg including data from (Bekoff, 1977; Berta, 1982; Burnie, 2005; de Waal, 2017; Dietz, 1984; Geptner et al., 1988; Hoffman, 2014; Hunter, 2019; Viranta et al., 2017). B) Scaling of tail index (TI) versus body mass in kg across multiple species (Bekoff, 1977; Berta, 1982; Burnie, 2005; de Waal, 2017; Dietz, 1984; Geptner et al., 1988; Hoffman, 2014; Hunter, 2019; Viranta et al., 2017). Silhouettes from Phylopic open source collection.

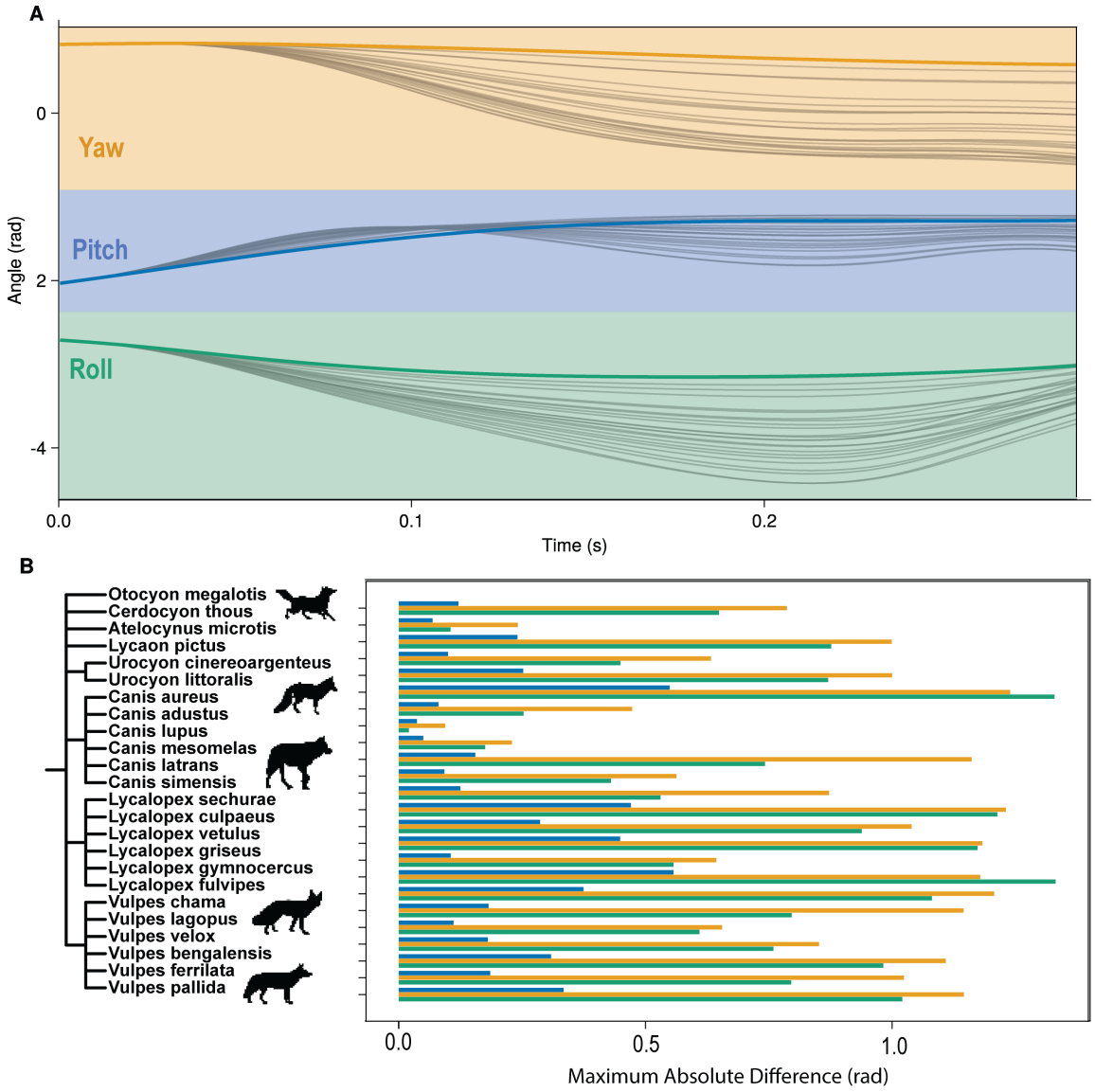

Figure 4: A) Scaling of pitch (blue), yaw (yellow), and roll (green) of $n = 24$ canidae species across simulation time of 0.293s. B) the phylogenetic tree of canidae species run through simulation with, C) their respective maximum absolute difference angle given by Equation (5) (green), Equation (4) (blue) , Equation (3) (yellow). Silhouettes from Phylopic open source collection.

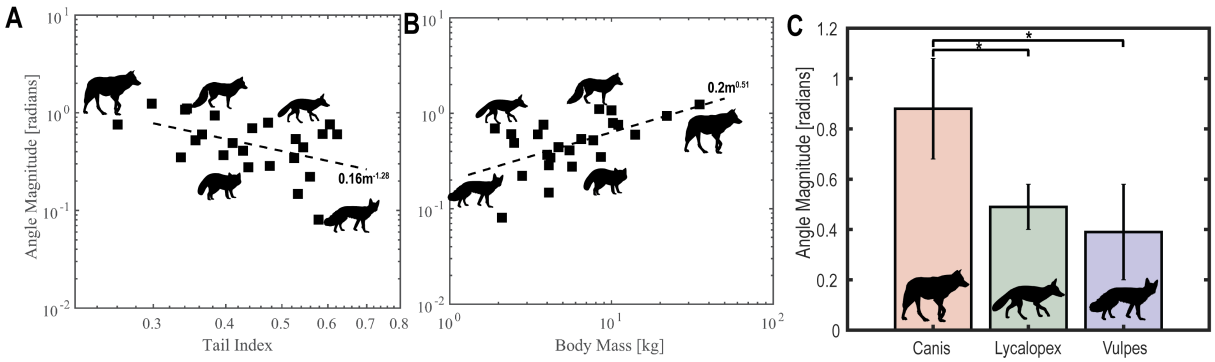

Figure 5: A) Scaling of Angle Magnitude (θ) across varying tail index (Equation (1)) of $n = 24$ extant *Canidae* species. B) Scaling of Angle Magnitude (θ) across varying Body Mass, in kg, of $n = 24$ extant *Canidae* species. C) Angle Magnitude (θ) of three different sub-families of the *Canidae* tree including *Canis, Lycalopex,* and *Vulpes*. Silhouettes from Phylopic open source collection.